JOURNAL OF CATALYSIS 93, 231–245 (1985)

Temperature-Programmed Reduction of Al_2O_3-, SiO_2-, and Carbon-Supported Re_2O_7 Catalysts

P. ARNOLDY,[1] E. M. VAN OERS,* O. S. L. BRUINSMA, V. H. J. DE BEER,* AND J. A. MOULIJN

*Institute for Chemical Technology, University of Amsterdam, Plantage Muidergracht 30, 1018 TV Amsterdam, The Netherlands, and *Laboratory for Inorganic Chemistry and Catalysis, Eindhoven University of Technology, P.O. Box 513, 5600 MB Eindhoven, The Netherlands*

Received March 9, 1984; revised June 11, 1984

Temperature-Programmed Reduction (TPR) has been applied to characterize the reducibility of Al_2O_3-, SiO_2-, and carbon-supported Re_2O_7 catalysts, over a wide range of transition metal content. Dried catalysts are found to contain a so-called monolayer-type Re^{7+} surface phase as well as crystalline NH_4ReO_4. Calcination at 575 or 825 K resulted in decomposition of NH_4ReO_4, formation of the Re^{7+} surface phase and Re_2O_7 clusters, and Re loss via sublimation of Re_2O_7. Differences in reducibility of the various catalyst samples are ascribed to variations in the strength and the heterogeneity of the Re^{7+}–support interaction. The strength of the interaction was found to depend on the support material applied and decreased in the order: $Al_2O_3 > SiO_2 >$ carbon. The heterogeneity was essentially the same for all three supports. The largely varying literature data on the reducibility of Re_2O_7/Al_2O_3 catalysts is supposedly related with the presence of additives, such as chlorides, which may increase the Re^{7+}–support interaction.

INTRODUCTION

Rhenium catalysts have several interesting properties. They show high activity for metathesis (*1, 2*), hydrodesulfurization (HDS) (*3–6*), and hydrodenitrogenation (*7*), in comparison with Mo and W catalysts. Re also increases the stability of Pt reforming catalysts (*8–11*) and, for a large range of organic syntheses, Re appears to be a selective hydrogenation catalyst (*12*).

The present study describes the reducibility, as measured by Temperature-Programmed Reduction (TPR), of Al_2O_3-, SiO_2-, and carbon-supported Re_2O_7 catalysts as a function of Re content and calcination conditions. The TPR technique was chosen for two reasons. First, TPR provides information on the reducibility, as such, over a wide range of temperatures. Second, TPR patterns give indications on the structure of catalysts, e.g., on the presence of crystallites and on the metal–oxygen bond strength.

Detailed information on the reducibility, as such, is important, because catalytically active Re sites are only created by reduction of the Re^{7+} ions, generally present in freshly prepared catalysts, to lower valencies, as occurs in the formation of Re carbenes (metathesis) (*13*), ReS_2 (HDS) (*3*), or Re metal (hydrogenation, reforming). Studies carried out on the reduction of Re^{7+} by H_2 mainly deal with reforming catalysts. Initially, reduction has been studied isothermally (*14, 15*). Subsequently, the TPR method (*16*) has been used frequently (*4, 17–22*). It is well established now that reduction results in conversion of Re^{7+} to Re metal in a narrow temperature range. However, as will be shown in the present study, the reported reduction temperatures vary to a large extent. It was thought that a more systematic study of the reduction of supported Re_2O_7 catalysts might reveal the origin of the inconsistencies in the literature data.

The present TPR study is also part of a

[1] Present address: Koninklijke/Shell Laboratorium, Badhuisweg 3, 1031 CM Amsterdam, The Netherlands.

0021-9517/85 $3.00

larger investigation which has the objective to correlate the HDS activity of sulfided Re catalysts with the structure of the oxidic precursor systems (*5*). The latter project focuses on the influence of type of support, by analogy with recent work on the reducibility and HDS activity of Al_2O_3-, SiO_2-, and carbon-supported Mo and W catalysts (*4, 23, 24*).

EXPERIMENTAL

a. Materials

NH_4ReO_4 (Drijfhout, "for analysis") and ReO_3 (ICN), being XRD-pure, were used as received. Re_2O_7 was prepared *in situ* by oxidation of ReO_3 in dry air followed by purification via sublimation. The following support materials were applied: High-purity γ-Al_2O_3 (Ketjen 000-1. 5E (CK 300), specific surface area 195 m^2/g, pore volume 0.50 cm^3/g, particle size 100–150 μm, chlorine content 0.04 wt%); SiO_2 (Grace 62, specific surface area 350 m^2/g, pore volume 1.05 cm^3/g, particle size 160–210 μm); and activated carbon (Norit RO-3, specific surface area 1000 m^2/g, pore volume 0.8 cm^3/g, particle size 175–300 μm). The activated-carbon support was purified by a treatment with boiling HCl (1 h), followed by washing with boiling H_2O and drying in air (16 h, 380 K). The remaining impurity level was low; X-ray fluorescence showed presence of chlorine, sulfur, and silicon.

b. Catalyst Preparation

The supported Re catalysts were prepared by pore volume impregnation of dried supports with solutions of NH_4ReO_4 in demineralized H_2O. The samples so obtained were dried, in air at 1 bar, by heating to 380 K at a rate of 20 K/h, followed by a 16-h isothermal period at 380 K. In some cases a 0.5-h calcination was applied, at 575 or 825 K. The medium used was air for Al_2O_3- and SiO_2-supported systems, whereas it was air (at 575 K) or Ar (at 575 or 825 K) for carbon-supported systems. The gases were purified in order to prevent carbon deposition on the catalysts. The Re content was varied drastically. High-loading catalysts were prepared by repeated pore volume impregnation and drying. Table 1 gives the Re content of the dried catalysts and also shows for which samples the presence of crystalline NH_4ReO_4 was established by means of XRD and TPR analysis. The catalysts are denoted as Re(x)/y, with x representing the theoretical Re content, expressed as the number of Re atoms per square nanometer support surface area (at./nm^2), and y representing the support material using the abbreviations Al, Si, and C for the Al_2O_3, SiO_2, and carbon supports, respectively. Atomic absorption spectrometry (Perkin–Elmer 300 AAS) was applied to check the theoretical Re content of dried catalysts (see Table 1) and to measure the Re loss due to calcination (see Table 2).

c. X-Ray Diffraction (XRD)

XRD has been carried out in a Philips diffractometer PW 1050/25 using Cu$K\alpha$ radiation. A Ni filter was applied to remove Cu$K\beta$ radiation. Crystallite sizes have been calculated using the Scherrer equation with correction for natural line broadening and assuming that the crystallite-shape factor K equals 1 (*25*).

d. Temperature-Programmed Reduction (TPR)

The TPR equipment has been described in detail elsewhere (*26*). A high-purity mixture of 67% H_2/Ar (flow rate 12 μmol/s; 1.0 bar) was used. In some cases this mixture was saturated with H_2O at room temperature, resulting in 2.6% H_2O in the reducing mixture. In a typical TPR experiment the heating rate was 10 K/min and the catalyst sample contained 2–5 μmol Re. The sample size was varied reciprocally with heating rate. H_2O, NH_3, CO_2, and organics (except CH_4), which evolved during reduction, were trapped in 3A and 5A molecular sieve columns. H_2 consumption as well as CH_4, CO, and O_2 production were measured as a positive peak by means of a thermal con-

TABLE 1

Dried Catalysts

Catalyst notation[a]	Theoretical Re content (wt% Re)[b]	Number of impregnation steps	Re content (AAS)[c] (at./nm^2)	Crystalline NH_4ReO_4[d]		Crystallite size[c,e] of NH_4ReO_4 (nm)
				(TPR)	(XRD)	
Re(0.0097)/Al	0.058	1	n.m.	−	−	n.m.
Re(0.025)/Al	0.147	1	n.m.	−	−	n.m.
Re(0.049)/Al	0.29	1	n.m.	−	−	n.m.
Re(0.097)/Al	0.58	1	n.m.	−	−	n.m.
Re(0.24)/Al	1.44	1	0.19	−	−	n.m.
Re(0.49)/Al	2.8	2	0.41	−	−	n.m.
Re(0.97)/Al	5.4	4	0.91	+	+	130
Re(2.43)/Al	12.1	10	2.61	+	+	260
Re(0.010)/Si	0.108	1	n.m.	−	−	n.m.
Re(0.025)/Si	0.27	1	n.m.	−	−	n.m.
Re(0.050)/Si	0.54	1	n.m.	−	−	n.m.
Re(0.10)/Si	1.07	1	n.m.	−	+	70
Re(0.25)/Si	2.6	1	0.24	+	+	110
Re(0.50)/Si	5.0	2	0.49	+	+	170
Re(1.00)/Si	9.4	3	0.97	+	+	170
Re(2.50)/Si	19.5	7	2.85	+	+	200
Re(0.0080)/C	0.25	1	n.m.	−	−	n.m.
Re(0.040)/C	1.22	1	n.m.	−	−	n.m.
Re(0.20)/C	5.7	1	n.m.	+	−	n.m.
Re(0.38)/C	10.7	2	0.36	+	−	n.m.
Re(0.80)/C	18.2	4	0.73	+	+	n.m.

[a] Theoretical Re content (at./nm^2) is given in parentheses; Al, Si and C refer to Al_2O_3, SiO_2, and carbon, respectively.

[b] Re is assumed to be present in the stoichiometry NH_4ReO_4.

[c] n.m. = not measured.

[d] The presence or absence of crystalline NH_4ReO_4, derived from TPR and XRD data, is indicated by a plus and a minus sign, respectively.

[e] Calculated from XRD results.

TABLE 2

Effect of Calcination in Air on the Re Content

Catalyst notation[a]	Re content[b] after drying (380 K) (at./nm^2)	Re content[b] after calcination (575 K) (at./nm^2)	Re content[b,c] after calcination (825 K) (at./nm^2)
Re(0.49)/Al	0.42	0.39	n.m.
Re(0.97)/Al	0.91	0.81	n.m.
Re(2.43)/Al	2.61	2.45	n.m.
Re(0.50)/Si	0.49	0.49	0.46
Re(1.00)/Si	0.97	0.94	0.93
Re(2.50)/Si	2.85	2.46	1.63
Re(0.38)/C	0.36	0.36	n.m.
Re(0.80)/C	0.73	1.20	n.m.

[a] For catalyst notation see footnote of Table 1.

[b] Measured by AAS.

[c] n.m. = not measured.

ductivity detector (TCD). A flame ionization detector (FID) was used for CH_4 detection only. CH_4 and CO were retarded by the 5A molecular sieves, to an extent which depended on the H_2O content of the zeolite surface. The retardation times for CH_4 and CO were 2.5 and 4.2 min, respectively (for TPR measurements on reference compounds and Al_2O_3- or SiO_2-supported catalysts), or 4.5 and 18 min, respectively (for TPR measurements on carbon-supported catalysts). Since the TPR patterns shown in Figs. 1–9 have not been corrected for these retardations, the CH_4 production peak is situated at a somewhat too high temperature (with a heating rate of 10 K/min and a retardation time of 2.5 min the peak shift is about 25 K).

RESULTS

a. X-Ray Diffraction

The Al_2O_3- and SiO_2-supported catalysts show very broad XRD lines of γ- or η-Al_2O_3 and α-crystobalite, respectively. The carbon-supported catalysts show very broad XRD lines at *d* values around 210 and 370 pm, which are typical for activated carbon; moreover, sharper lines are observed at *d* values of 335 (graphite impurities) and 405 pm (origin unknown). Depending on the type of support and the Re content some dried catalysts show NH_4ReO_4 lines, superimposed on the support pattern (see Table 1). Dried Re(0.0097–0.49)/Al samples do not show any NH_4ReO_4 lines; for dried Re(0.97)/Al, sharp NH_4ReO_4 lines of low intensity are observed (crystallite size 130 nm), while for dried Re(2.43)/Al these lines are of much higher intensity (crystallite size 260 nm). Dried Re(0.10–2.50)/Si catalysts show sharp NH_4ReO_4 lines, the intensity of which increases regularly with increasing Re content, whereas the crystallite size increases from 70 to 200 nm. For carbon-supported catalysts NH_4ReO_4 lines, of very low intensity, are observed only for the dried Re(0.80)/C sample. Calcination of Al_2O_3-, SiO_2-, and carbon-supported catalysts at 575 or 825 K leads to disappearance of the NH_4ReO_4 lines, with the exception of Re(2.50)/Si. In the latter case, after calcination at 575 K, NH_4ReO_4 lines are still present, although they are reduced sharply in intensity. Besides NH_4ReO_4- and support-lines, both dried and calcined Re(0.25–2.50)/Si catalysts show additional lines of low intensity with *d* values of 318 and 486 pm. These lines could not be assigned to Re_2O_7 (*27*), $Re_2O_7 \cdot 2H_2O$ (*28*), nor to any Re compound included in the ASTM system, but for obvious candidates, namely Re silicates, no ASTM data are available.

b. Colors

All Al_2O_3-supported catalysts are white, independent of calcination temperature. SiO_2-supported catalysts are white after drying. Calcination at 575 K changes the color to light grey–blue (Re(0.25)/Si), dark grey–blue (Re(0.50)/Si), and black (Re(1.00–2.50)/Si). Calcination at 825 K leads to recovery of the white color. In separate experiments, in which the Re(2.50)/Si sample was calcined in air at various temperatures, it is observed that coloring starts around 500 K. The color disappears around 600 K, while simultaneously Re_2O_7 sublimation takes place.

c. Temperature-Programmed Reduction

Figures 1–9 show the TPR data. In all TPR patterns the Re reduction peaks are sharp, while quantitative analysis of TPR results generally indicates a single-step reduction from Re^{7+} (Re^{6+} in the case of ReO_3) to Re^0. Once Re^0 is formed, considerable CH_4 production is found in most cases, due to reduction of organic impurities, adsorbed on Re catalysts and on the quartz wool plugs around the samples. About 1.2 mol H_2 per CH_4 is consumed, in agreement with the conclusion drawn previously that these organics consist of (polymerized) acetone (*26*).

Figure 1 shows the TPR patterns of crystalline reference compounds. The reducibility increases in the order: NH_4ReO_4 <

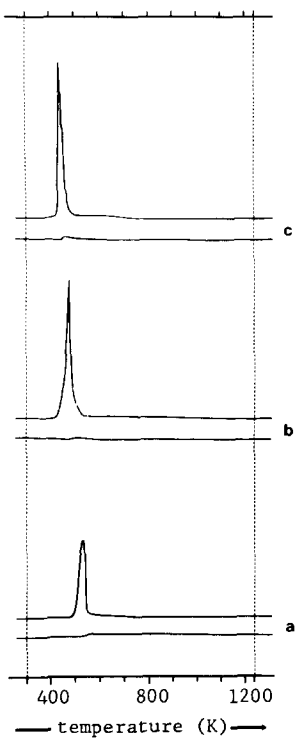

FIG. 1. TPR patterns (1 K/min) of reference compounds: (a) NH_4ReO_4, (b) Re_2O_7, (c) ReO_3. The upper and lower part of each pattern represent the TCD and FID signals, respectively.

$Re_2O_7 < ReO_3$. For TPR analysis of NH_4ReO_4 and ReO_3 exceptionally small samples have been used (ca. 5 μ-mol Re at a heating rate of 1 K/min); larger samples (especially in the case of NH_4ReO_4) showed TPR peak broadening toward higher temperatures due to inhibition of reduction by NH_3 or H_2O. For Re_2O_7 the influence of sample size on TPR has not been checked because of its time-consuming *in situ* preparation procedure. In order to limit Re_2O_7 sublimation (*29*) during TPR analysis, the crystalline compounds were heated at a rate of 1 K/min. TPR of Re_2O_7 at 10 K/min shows the reduction maximum at higher temperature (565 K) and a significant sublimation of Re_2O_7, in agreement with literature (*17*).

Figure 2 gives a survey of the position of the TPR peak maxima (T_{max}), due to reduction of Re ions in supported Re catalysts. T_{max} values are given as a function of support, calcination, and Re content. The corresponding TPR patterns (10 K/min) are shown in the Figs. 3 and 5–9. For all three supports two lines can be drawn:

(i) Most peaks observed in the range 540–560 K for dried catalysts with high Re contents are assigned to reduction of NH_4ReO_4 crystallites (see also Table 1).

(ii) All other peaks, found over the temperature range 510–730 K, are assigned to reduction of Re^{7+} surface ions which interact with the support.

The NH_4ReO_4 reduction peak has its T_{max} value at slightly lower temperatures in the case of carbon-supported catalysts (540 K) than in the case of Al_2O_3- or SiO_2-supported catalysts (560 K), probably due to the different crystallite sizes involved. NH_4ReO_4

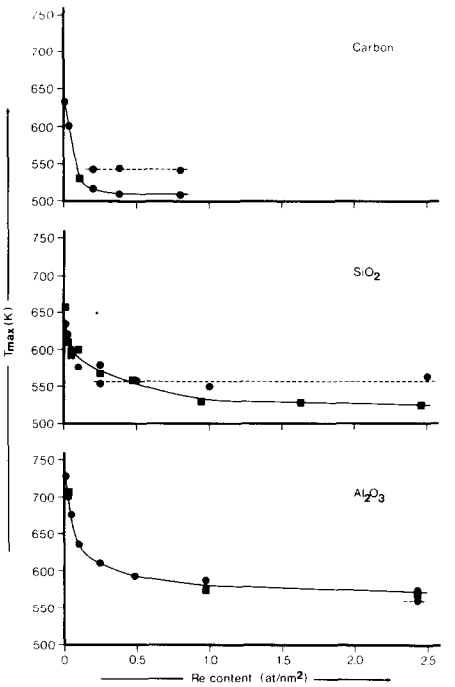

FIG. 2. Survey of the position of the Re reduction peak maxima (T_{max}), at 10 K/min, as a function of Re content of catalysts supported on Al_2O_3, SiO_2, or carbon, which are dried at 380 K (circles) or calcined at 575 or 825 K (squares). The dotted lines represent reduction of NH_4ReO_4 crystallites; the full lines represent reduction of Re^{7+} surface species.

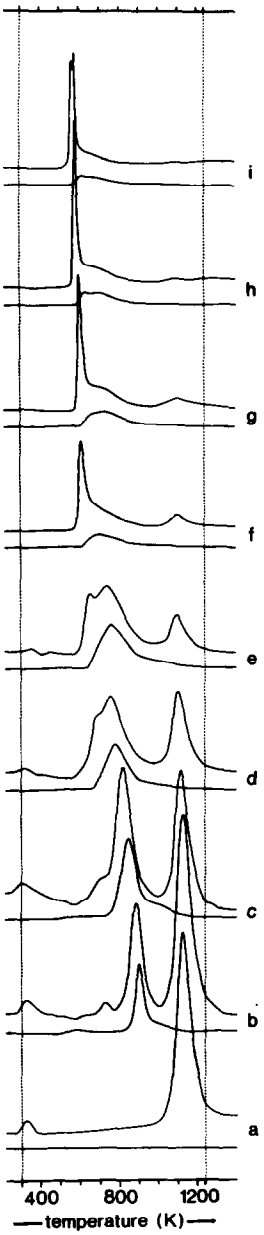

FIG. 3. TPR patterns (10 K/min) of dried Re_2O_7/Al_2O_3 catalysts having the following Re contents (at./nm^2): (a) 0, (b) 0.0097, (c) 0.025, (d) 0.049, (e) 0.097, (f) 0.24, (g) 0.49, (h) 0.97, (i) 2.43. The upper and lower part of each pattern represent the TCD and FID signals, respectively.

crystallites are observed at much lower Re content for SiO_2- and carbon-supported than for Al_2O_3-supported catalysts. Calcination results in decomposition of NH_4ReO_4 and formation of more Re^{7+} surface species, but does not significantly change the reduction temperature of the surface species. The T_{max} values for reduction of Re^{7+} surface species decrease with increasing Re content for all supports, but are higher for Al_2O_3-supported than for SiO_2- or carbon-supported catalysts over the entire Re loading range studied. The shape of the curves shown in Fig. 2 for the latter reduction is different for each support, whereas the total shift of T_{max} is only slightly larger for Al_2O_3-supported than for SiO_2- or carbon-supported catalysts, namely ca. 155 and 125 K, respectively.

Besides Re^{7+} reduction, the TPR patterns of supported catalysts show also other common features:

(i) Just above room temperature, a peak is found which is probably caused by O_2 desorption from the support surface.

(ii) Production of CH_4 (FID) and H_2 (negative TCD signal) in the range 400–650 K indicates that some cracking of organic impurities occurs at temperatures where Re^0 is not yet formed (see Figs. 3b–e and 6b–c).

(iii) CH_4 production peaks, due to reduction of organic impurities, are found in the range 580–870 K and shift to lower temperature with increasing Re content, apparently due to the concomitant shift of the Re^{7+} reduction peaks to lower temperature which results in Re^0 formation.

(iv) In the high-temperature part of the TPR patterns, each support is found to have a characteristic TPR pattern.

Figure 3 shows the TPR patterns of dried Al_2O_3-supported catalysts as a function of Re content. At low Re contents the TPR patterns are dominated by peaks which are not related to reduction of Re ions. Besides CH_4 production, a peak near 1100 K is found, assigned to reduction of Al_2O_3 impurities, such as iron, sulfite, and sulfate (*26*). The latter shifts ca. 50 K to lower temperatures with increasing Re content, suggesting that this reduction is catalyzed by Re.

Figure 4 shows the TCD part of the TPR patterns obtained for dried Al_2O_3-supported

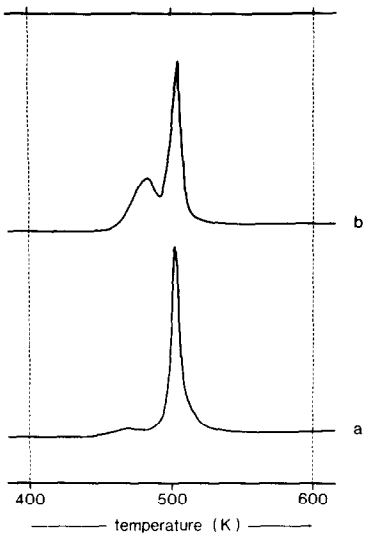

FIG. 4. TPR patterns (0.2 K/min) of dried Re_2O_7/Al_2O_3 catalysts having the following Re contents (at./nm^2): (a) 0.97, (b) 2.43. Only the TCD part of the patterns is shown.

catalysts having the two highest Re contents. Note that, in this case, the heating rate was 0.2 instead of 10 K/min. Clearly two peaks are present, one around 505 K due to reduction of Re^{7+} surface ions and another at about 475 K caused by reduction of NH_4ReO_4 crystallites. At the lower heating rate (0.2 K/min) these peaks are better resolved and the distribution of Re^{7+} over the two phases can be calculated easily. Approximately 9 and 40% of the Re ions is present as NH_4ReO_4 crystallites, corresponding to a concentration of Re^{7+} surface phase of about 0.88 and 1.46 at./nm^2 in the dried Re(0.97)/Al and Re(2.43)/Al catalyst, respectively. Separate TPR experiments showed that the NH_4ReO_4 TPR peak intensity decreases slightly with increasing heating rate, due to some decomposition of NH_4ReO_4 during TPR.

Figure 5 shows the TPR patterns of Re(2.43)/Al as a function of calcination temperature. Calcination leads to disappearance of the NH_4ReO_4 reduction peak and to a 10 K shift of the peak due to reduction of the remaining Re^{7+} surface phase to lower temperature. The latter effect has also been found for the other Re/Al samples. In order to check the possible influence of H_2O on the reducibility, some TPR analyses of dried Re(0.97)/Al have been executed using H_2O-saturated H_2/Ar as reducing mixture. The addition of H_2O causes a shift of ca. 10 K to higher temperature for the peak due to reduction of Re^{7+} surface ions.

For the Al_2O_3-supported catalysts no Re_2O_7 deposition has been observed in colder parts of the calcination reactor, showing that no Re loss takes place during calcination. AAS- and quantitative TPR-results are in agreement with this.

Figure 6 shows the TPR patterns of dried SiO_2-supported catalysts as a function of Re content. Besides Re^{7+} reduction and CH_4 production, a reduction pattern is observed between 800 and 1200 K, which is

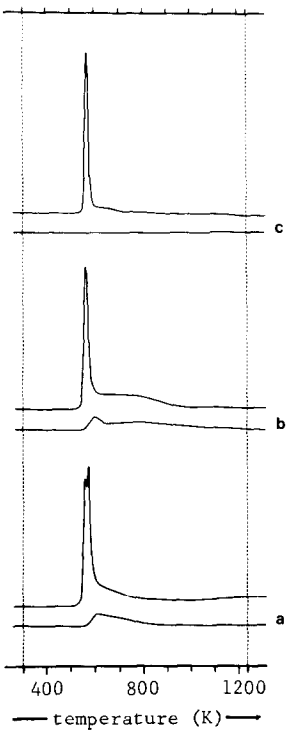

FIG. 5. TPR patterns (10 K/min) of the Re(2.43)/Al catalyst as a function of calcination temperature: (a) 380 K (drying), (b) 575 K, (c) 825 K. The upper and lower part of each pattern represent the TCD and FID signals, respectively.

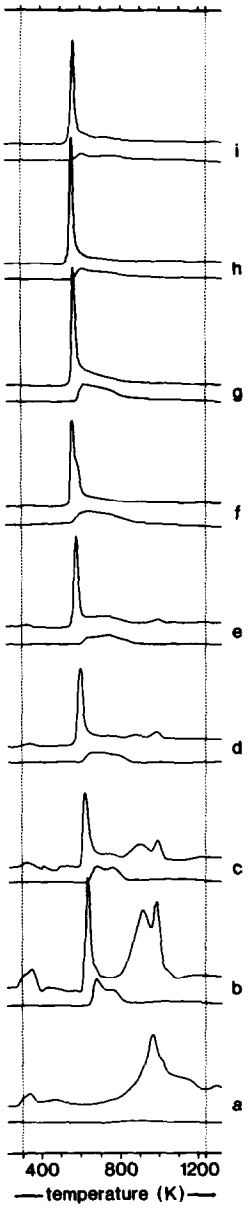

FIG. 6. TPR patterns (10 K/min) of dried Re_2O_7/SiO_2 catalysts having the following Re contents (at./nm^2): (a) 0, (b) 0.010, (c) 0.025, (d) 0.050, (e) 0.10, (f) 0.25, (g) 0.50, (h) 1.00, (i) 2.50. The upper and lower part of each pattern represent the TCD and FID signals, respectively.

typical for the SiO_2 support. As in the Al_2O_3 case, it is assigned to reduction of impurities. Again, one concludes that Re catalyzes this reduction, since its presence causes the appearance of a second distinct maximum in the SiO_2 reduction pattern as well as a shift to lower reduction temperatures.

Figure 7 shows the TPR patterns of Re(2.50)/Si as a function of calcination temperature. AAS and quantitative TPR analysis show that Re loss takes place, especially upon calcination at 825 K. Calcination results in some TPR peak broadening; this is also observed for Re(0.50–1.00)/Si. At lower Re contents no significant calcination effects are observed.

Figure 8 shows the TPR patterns of dried carbon-supported catalysts as a function of Re content. The Re reduction peaks are small compared with those caused by gasification of the support. Three different gasification regions can be discerned, in the broad temperature range of 500–1240 K:

1. The first region (500–900 K) represents pyrolysis of the activated carbon. At low Re content this is observed as production of

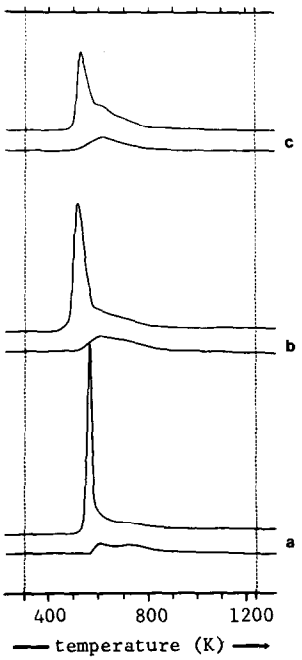

FIG. 7. TPR patterns (10 K/min) of the Re(2.50)/Si catalyst as a function of calcination temperature: (a) 380 K (drying), (b) 575 K, (c) 825 K. The upper and lower part of each pattern represent the TCD and FID signals, respectively.

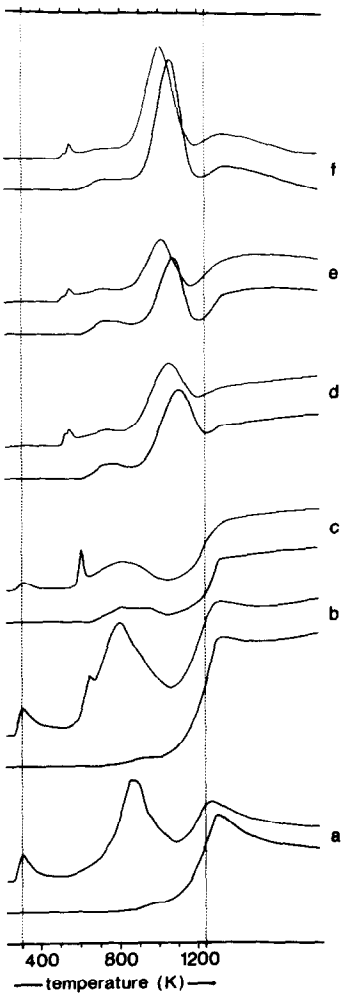

FIG. 8. TPR patterns (10 K/min) of dried Re_2O_7/carbon catalysts having the following Re contents (at./nm^2): (a) 0, (b) 0.0080, (c) 0.040, (d) 0.20, (e) 0.38, (f) 0.80. The upper and lower part of each pattern represent the TCD and FID signals, respectively.

CO and consumption of H_2 (CO_2 and H_2O production cannot be detected in the TPR apparatus). At higher Re contents CH_4 production dominates; this CH_4 probably is formed from the primary pyrolysis products CO and CO_2, since it was shown in separate experiments that CO and CO_2 are converted quantitatively to CH_4 over Re^0 centers, under the TPR conditions applied.

2. The second region (900–1100 K) can only be distinguished in the TPR patterns recorded for the Re(0.20–0.80)/C catalysts as a relatively sharp peak which is associated with strongly catalyzed gasification. Apparently this type of gasification is deactivated fast at temperatures around 1100 K.

3. The third region (above 1100 K) represents weakly catalyzed gasification. During the isothermal reduction stage some activation of this type of catalysis occurs at low Re contents, whereas at higher Re contents an activity decrease is observed, probably due to carbon shortage at high burn-off.

Re-catalyzed gasification has hardly been studied (*30*). More work has been done on the Ni-catalyzed gasification (*31–33*). Re and Ni seem to act similarly in catalytic gasification. Accordingly, it is proposed that gasification in the second region is catalyzed by Re^0 crystallites. The deactivation observed at the high-temperature side of this region might be caused by carbon deposition on the Re^0 phase, by Re carbide formation or by loss of dispersion because of Re^0 crystallite growth. The remaining gasification activity observed in the third region is then associated with (partially) covered Re^0 crystallites or with Re carbide. Redispersion of these Re phases assumedly accounts for the reactivation of gasification in the isothermal reduction stage.

Figure 9 shows the TPR patterns of Re(0.20)/C as a function of calcination temperature and medium. Calcination at 575 and 825 K leads to decomposition of NH_4ReO_4 followed by significant Re_2O_7 sublimation (40 and 55% Re loss, respectively), but does not affect gasification in region two and three. This can be explained assuming that NH_4ReO_4 crystallites are precursors of relatively large Re^0 crystallites having a low gasification activity. The increase of Re content upon calcination, especially for the Re(0.80)/C catalyst (see Table 2), shows that also carbon loss takes place, obviously via catalytic oxidation. Moreover, the oxygen content of the carbon is influenced by the calcination medium, since calcination in air and Ar lead to an increase and decrease of pyrolysis activity, respectively. The small peak at 475 K,

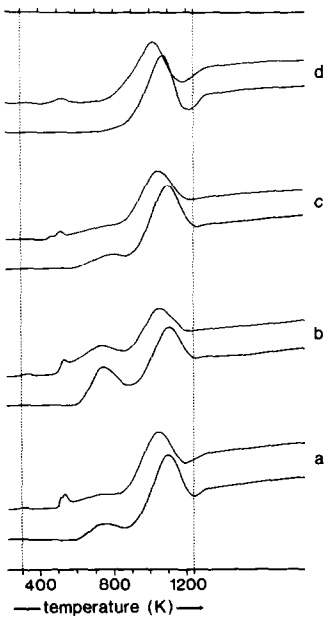

FIG. 9. TPR patterns (10 K/min) of the Re(0.20)/C catalyst as a function of temperature treatment and medium: (a) 380 K, air (drying), (b) 575 K, air, (c) 575 K, Ar, (d) 825 K, Ar. The upper and lower part of each pattern represent the TCD and FID signals, respectively.

observed only after heating at 575 K in Ar, is assigned to reduction of some partly reduced Re phase, e.g., ReO_3 crystallites.

DISCUSSION

a. Preparation and Structure of Oxidic Re Catalysts

All TPR patterns reported here show sharp peaks connected with a one-step reduction of high-valent Re ions with formation of mainly Re^0. The sharpness of the peaks suggests strongly that autocatalysis plays an important role in the reduction mechanism (*34*). In agreement with this, it has been reported that reduction of Re^{7+} can be accelerated by the presence of Re^0 and Pt^0 (*17, 20*). In addition, if autocatalysis is indeed an important factor, it can be easily understood why the observed reduction peaks are sharper than one would expect on the grounds of peak width calculations, carried out assuming that the reducibility of a Re catalyst is the sum of intrinsic reducibilities of all Re ions present (for this calculation the curves of Fig. 2 can be used). Finally, for Al_2O_3-supported catalysts the activation energy value for reduction of Re^{7+} surface species is only slightly higher than the value for reduction of NH_4ReO_4 crystallites (111 versus 95 kJ/mol), again suggesting autocatalysis (*35*).

Dried catalysts. TPR shows the presence of NH_4ReO_4 crystallites in dried catalysts. Generally the TPR data agree well with the XRD data with respect to the presence of NH_4ReO_4 (see Table 1). Except for Re(0.10)/Si, which contains a very small fraction of crystalline NH_4ReO_4, TPR is more sensitive than XRD; TPR has the advantage of enabling both detection of small crystallites, such as are present in Re(0.20–0.80)/C samples, and quantification of the fraction of crystalline material formed.

By means of quantitative TPR analysis, the capacity of the supports to bond ReO_4^- ions during impregnation and drying, with formation of Re^{7+} surface species, is determined to be 0.05, 0.05, and 0.8 at./nm^2 for carbon, SiO_2, and Al_2O_3, respectively. The SiO_2 and carbon values are very small. However, even in the Re/Al case, the capacity is small in comparison with the monolayer capacity of 3.3 at./nm^2 obtained for calcined catalysts (*36*). The strength of the interaction of ReO_4^- ions with the Al_2O_3 (and the NH_4ReO_4) lattice might be similar, leading to competition between formation of Re^{7+} surface species and NH_4ReO_4 crystallites. The formation of the Re^{7+} surface phase during impregnation and drying can probably be favored by adjustment of the pH of the impregnation solution to lower values, in order to increase the positive charge density at the support surface (*37, 38*).

The fact that the carbon-supported NH_4ReO_4 crystallites could not be detected by XRD implies that their size is small (<3 nm). For the Al_2O_3- and SiO_2-supported catalysts, however, very large NH_4ReO_4 crystallites have been found (ca. 100 nm).

This striking difference between carbon, on the one hand, and Al_2O_3 and SiO_2, on the other hand, is explained tentatively considering the construction of their pore systems. In the case of Al_2O_3 and SiO_2 meso- and macropores are usually interconnected, resulting in easy formation of NH_4ReO_4 crystallites in the macropores, by transport of ReO_4^- ions from nearby mesopores. In the case of activated carbon, the abundantly present micropores as well as the mesopores are longer and generally not directly connected with the macropores (*39*). As a result, ReO_4^- ions cannot migrate from the narrow pores during drying and only small crystallites can be formed. Therefore, it is concluded that activated carbon is an excellent support to create small crystallites.

Calcined catalysts. Calcination at 575 or 825 K leads to decomposition of NH_4ReO_4 crystallites with formation of Re_2O_7 which sublimes under the calcination conditions applied (*29*) when no interaction with the support takes place. Calcination of Al_2O_3-supported catalysts leads, without Re loss, to formation of a Re^{7+} surface phase of the so-called monolayer-type (*36*). Apparently, the Re ions originating from large NH_4ReO_4 crystallites present in the macropores have moved into the mesopores. In order to explain this Re^{7+} mobility two possibilities suggest themselves. Surface migration cannot be excluded, but is not very likely to occur in view of the high charge of the Re ions and the important Re^{7+}–Al_2O_3 interaction. Probably Re ions are transported as gas-phase Re_2O_7, which rapidly transforms into monolayer Re^{7+} species upon collision with the Al_2O_3 surface. In this way Re loss via the gas phase is efficiently blocked.

SiO_2-supported catalysts show a more complicated behavior upon calcination. Again decomposition of NH_4ReO_4 crystallites causes an increase in Re dispersion, but now also Re loss takes place via gas-phase Re_2O_7, especially during calcination of the Re(2.50)/Si sample at 825 K (see Table 2). The dark colors observed after calcination at 500–600 K are reminiscent of the deep green–blue color observed for solid Re_2O_7, which is slightly reduced by H_2O-assisted oxygen loss, suggesting the presence of small Re_2O_7 clusters on SiO_2-supported catalysts with high Re content. Considering the small Re loss due to calcination at 575 K, the clusters are probably stabilized by the support, which is only compatible with the presence of very small-sized clusters. They are probably formed at ca. 500–600 K from large NH_4ReO_4 crystallites, via gas-phase Re_2O_7, and decompose above ca. 600 K with formation of gas-phase Re_2O_7 once more. It is concluded that SiO_2-supported catalysts can obtain two kinds of Re^{7+} surface species, namely small Re_2O_7 clusters as well as monolayer-type Re^{7+} surface species. For the Re(2.50)/Si sample a surface coverage of 1.6 at./nm^2 results after calcination at 825 K, which value is postulated as the monolayer capacity of calcined SiO_2-supported Re catalysts.

The unknown XRD lines at d values of 318 and 486 pm, observed in the diffractograms of both dried and calcined SiO_2-supported catalysts, may well be due to crystallites of a mixed Re–Si oxide (Re–silicate). The formation of these crystallites might be related to the hygroscopic nature of Re compounds such as Re_2O_7. Adsorption of H_2O is supposed to result in a liquid H_2O film in which Re^{7+} monolayer species and Re_2O_7 clusters dissolve, resulting in a low-pH solution. Subsequently, proton-catalyzed hydrolysis of the SiO_2 surface can take place, followed by crystallization of a Re-silicate from the solution. A separate scanning electron microscopic study supported this picture. The Re fraction present as large Re–silicate-type crystallites is estimated to be small, because a significant shift of T_{max} as a function of Re content is found (see Fig. 2) consistent with dominance of surface species. Moreover, no separate TPR peak has been observed for reduction of Re–silicate-type crystallites.

As for SiO_2-supported catalysts, Re loss is observed due to calcination of carbon-supported catalysts. An increase of calcination temperature from 575 to 825 K leads to an increase of Re loss for the Re(0.20)/C sample, suggesting that, on carbon as on SiO_2, Re_2O_7 clusters are present after calcination at 575 K. Heating at 575 K in Ar might lead to partial reduction of these clusters, while during heating at 825 K in Ar the Re loss as Re_2O_7 is supposed to be much faster than partial reduction. On the basis of the Re content of the Re(0.20)/C sample heated at 825 K in Ar, the monolayer capacity of heat-treated carbon-supported Re catalysts is estimated to be 0.1 at./nm^2. The much higher Re content of the Re(0.80)/C sample after calcination at 575 K in air is supposedly related to the presence of a large fraction of Re_2O_7 clusters, while also the oxygen content of the activated carbon can affect the monolayer capacity.

For all three supports studied the effect of calcination on catalyst structure is limited almost completely to decomposition of NH_4ReO_4 crystallites. No significant influence of calcination is found on the reducibility of Re^{7+} surface species which are already present on dried samples, showing that the same monolayer-type Re^{7+} surface species are present on both dried and calcined catalysts. No significant solid-state diffusion processes, leading to stronger Re^{7+}–support interaction, have taken place at elevated temperatures.

The small shift of T_{max} of the Re^{7+} surface phase reduction peak, due to calcination of Al_2O_3-supported catalysts, may arise from adsorbed H_2O (*22, 36*), which blocks some vacancies which are necessary for the initiation of reduction. The surprisingly small effect of the H_2O content on the T_{max} value has been reported before (*21*) and is confirmed in this study by the finding that intentional saturation of the H_2/Ar reducing mixture with H_2O leads to an upward T_{max} shift of only about 10 K.

The T_{max} value determined for the reduction of Re^{7+} surface species is considerably influenced by the Re content and the support choice (see Fig. 2). Differences in reducibility between Al_2O_3- and SiO_2-supported Re catalysts have been reported before (*15, 40*). The results of the present study are explained both by differences in interaction forces between Re^{7+} ions and the various supports and by heterogeneity of the interaction. The strength of the Re^{7+}–support interaction becomes noticeable in several ways: (i) the capacity of the supports for the uptake of ReO_4^- ions during impregnation and drying; (ii) the capacity of the supports for the formation of stable Re^{7+} surface species during calcination at 825 K (the monolayer capacity); and (iii) the T_{max} value of the Re^{7+} surface phase reduction peak for various supports at comparable Re content (at./nm^2).

Everything points to Al_2O_3 being the support which interacts strongest with Re^{7+} ions. SiO_2 exhibits stronger interaction than carbon, as can be easily seen from the differences in monolayer capacity.

Heterogeneity of the Re^{7+}–support interaction becomes evident from the shape of the curves shown in Fig. 2. Clearly a distribution of Re^{7+} ions over "stronger" and "weaker" sites has taken place. Remarkably, this is the case for all three supports to a comparable extent. It is shown elsewhere that, besides bond-energy factors, also entropy factors affect the observed heterogeneity (*35*).

b. Comparison with Literature Data for Re_2O_7/Al_2O_3 Reduction

A sharp Re reduction peak has also been found in all other studies on TPR of Re catalysts. Occasionally, a high-temperature contribution in the range 650–950 K is also reported (*4, 18, 22*). However, its assignment to Re reduction is questionable, because it may be present due to reduction of organic impurities.

The literature values of T_{max} for the Re^{7+} reduction peak vary over a wide range (550–880 K). As shown in Fig. 9, the T_{max} value is obviously dependent on Re con-

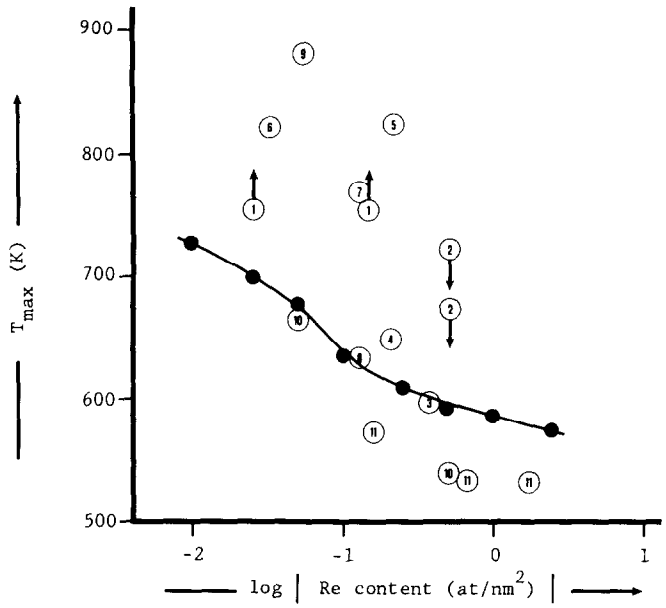

FIG. 10. Comparison of Re_2O_7/Al_2O_3 reducibility data (T_{max} of Re^{7+} surface phase); data for the dried catalysts from this study (closed circles plus full line) and various literature data (open circles with numbers included), as a function of Re content. The studies used are: 1 and 2, Refs. (*14, 15*), respectively (isothermal studies; the open circles indicate the reduction temperature chosen, while the arrows show where T_{max} is expected in case the experiments had been performed in the TPR mode); 3, Ref. (*17*); 4, Ref. (*18*); 5, Ref. (*18*), TPR after N_2 treatment at 775 K for 16 h; 6, Ref. (*19*); 7, Ref. (*20*); 8, Ref. (*20*), TPR after reduction–reoxidation; 9, Ref. (*21*); 10, Ref. (*4*); 11, Ref. (*22*).

tent. Therefore in Fig. 10 a survey of T_{max} values, taken from the present as well as from already published studies, is given as a function of Re content. Data taken from two isothermal reduction studies are also included. Slightly different experimental conditions have been applied in the assembled temperature-programmed studies. The spreading in H_2 pressure (0.05–1 bar) has to be accounted for, because it has been shown that T_{max} shifts more than 220 K to higher temperatures when the H_2 pressure is decreased by a factor of 1000 (*17*). The diversity in heating rates (4–10 K/min) is of minor importance, because it has been established that an increase of the heating rate by a factor of 10 leads to a 55 K upward shift of T_{max} (*35*). The results of the present study agree well with most literature data, taking into account the variations in H_2 pressure and heating rate as well as the use of different Al_2O_3 batches. However, in five references (*14, 18–21*) describing the reduction of catalysts with low Re content, T_{max} values have been reported which lie up to 200 K above the generally found values.

The following explanations will be considered:

First, it has been reported that pretreatment of Re_2O_7/Al_2O_3 catalysts with low Re content at high temperature in inert gas or under vacuum leads to prereduction of Re^{7+} to Re^{4+} (*18*). The resulting supported Re^{4+} ions reduce at much higher temperature than the original Re^{7+} ions, suggesting the formation of a rather stable compound between Re^{4+} oxides and Al_2O_3, via diffusion of Re^{4+} ions. This does not explain, however, why in references (*14, 19–21*), dealing with reduction of calcined Re^{7+} catalysts, also very high T_{max} values are reported.

A second possibility is that upon calcination very stable compound formation be-

tween Re^{7+} oxides and Al_2O_3 occurs, leading to structures having very high T_{max} values (*15, 16, 21*). The present study shows that calcination does not cause such an effect.

Also the H_2O concentration at the catalyst surface might influence the reducibility of Re^{7+} (*15, 19, 41*). Although the presence of H_2O has a tremendous effect on alloy formation and reducibility of Re^{7+} in Pt–Re/Al_2O_3 catalysts, it does not appear to be a critical factor in the monometallic Re catalysts (*21*). This is supported by our finding that TPR measurements using H_2O-saturated H_2/Ar did not result in a significant T_{max} shift.

A more suitable explanation might be found in the role of additives present on the Al_2O_3 support. Interestingly, in some references (*20, 21*) the presence of chloride is reported, whereas in others (*14, 19*) no attention is paid to possible additives such as chloride. Although it is shown that a decrease in chloride content by a factor of 10 does not influence the T_{max} value (*21*), the Cl/Re ratio after removal of chloride was still 1.3, which is high enough to allow the presence of a stoichiometric Re–Cl complex. Moreover, the catalyst applied contained also Pt leaving open the possibility of a Pt-catalyzed Re reduction camouflaging the influence of chloride. In another study (*20*) it is found that T_{max} for reduction of Re^{7+} is decreased after a reduction–reoxidation cycle, which might be due to loss of chloride (e.g., as HCl) during reduction. Also in the present study the Al_2O_3 support contains some chloride (0.04 wt%), leading to Cl/Re ratios above 1 for the Re(0.0097–0.025)/Al samples, which can explain part of the heterogeneity observed.

We therefore propose that additives such as chloride might modify the support locally, in such a way that very polar, strong Re^{7+} chemisorption sites are created resulting in very low Re^{7+} reducibility.

CONCLUSIONS

1. Under the TPR conditions applied, Re^{7+} ions reduce in a very narrow temperature range leading to sharp TPR peaks, most probably as a result of autocatalysis by instantly formed Re^0. Ultimately, Re^{7+} reduces to mainly Re^0. Reduction of organic impurities (probably polymerized acetone) is catalyzed by Re^0 and leads to CH_4 formation.

2. For dried catalysts TPR indicates the presence of both a Re^{7+} surface phase (of monolayer type) and NH_4ReO_4 crystallites. With respect to the detection of NH_4ReO_4 crystallites TPR has advantages over XRD: TPR can be used for quantitative analysis and for detection of very small crystallites.

3. Under the preparation conditions applied, the ReO_4^- adsorption capacity of Al_2O_3, SiO_2, and carbon during impregnation and drying is small.

4. Calcination at 575 or 825 K leads to decomposition of NH_4ReO_4 crystallites with formation of Re_2O_7. Depending on calcination temperatures, type of support, and transition metal content Re is redistributed over the surface or disappears from the catalyst sample. In both cases Re transport supposedly takes place via gas-phase Re_2O_7. Redistributed Re ions take part in monolayer formation or, in the case of limited monolayer capacity (SiO_2, carbon), form small Re_2O_7 clusters.

5. The reducibility mainly depends on Re content and support properties. The calcination temperature has only a small effect. The differences in reducibility are caused both by the strength of the Re^{7+}–support interaction, which decreases in the order $Al_2O_3 > SiO_2 >$ carbon, and by heterogeneity of this interaction, which is similar for the three supports.

6. TPR of carbon-supported Re catalysts shows three types of gasification. At 500–900 K pyrolysis of oxygen-containing groups takes place with production of CO and CO_2, which are converted easily to CH_4 over Re^0 under the TPR conditions applied. At 900–1100 K gasification is strongly catalyzed, probably by Re^0 crystallites. Above ca. 1100 K gasification is supposed to be only weakly catalyzed.

7. For Re_2O_7/Al_2O_3 catalysts containing

small amounts of Re, literature reduction data are inconsistent. Differences in the concentration of additives such as chloride might explain these variations.

ACKNOWLEDGMENTS

This study was supported by the Netherlands Foundation for Chemical Research (S.O.N.) with financial aid from the Netherlands Organization for the Advancement of Pure Research (Z.W.O.). Thanks are due to Dr. B. Koch and W. Molleman (Department of X-Ray Spectrometry and Diffractometry, University of Amsterdam), C. Bakker (Laboratory for Electron Microscopy, University of Amsterdam), and A. M. Elemans-Mehring (Atomic Absorption Spectrometry measurements, Laboratory for Inorganic Chemistry and Catalysis, Eindhoven University of Technology).

REFERENCES

1. Mol, J. C., and Moulijn, J. A., "Advances in Catalysis," Vol. 24, p. 131. Academic Press, New York, 1975.
2. Olsthoorn, A. A., and Boelhouwer, C., *J. Catal.* **44,** 207 (1976).
3. Pecoraro, T. A., and Chianelli, R. R., *J. Catal.* **67,** 430 (1981).
4. Thomas, R., van Oers, E. M., de Beer, V. H. J., Medema, J., and Moulijn, J. A., *J. Catal.* **76,** 241 (1982).
5. van Oers, E. M., Arnoldy, P., de Beer, V. H. J., Moulijn, J. A., and Prins, R., to be published.
6. Brooks, C. S., *Surf. Technol.* **10,** 379 (1980).
7. Stern, E. W., *J. Catal.* **57,** 390 (1979).
8. Kluksdahl, H. E., U.S. Patent 3.415.737 (1968).
9. Biloen, P., Helle, J. M., Verbeek, H., Dautzenberg, F. M., and Sachtler, W. M. H., *J. Catal.* **63,** 112 (1980).
10. Bertolacini, R. J. and Pellet, R. J., *in* "Catalyst Deactivation" (B. Delmon and G. F. Froment, Eds.), p. 73. Elsevier, Amsterdam, 1980.
11. Coughlin, R. W., Kawakami, K., Hasan, A., and Buu, P., *in* "Metal-Support and Metal-Additive Effects in Catalysis" (B. Imelik *et al.*, Eds.), p. 307. Elsevier, Amsterdam, 1982.
12. Davenport, W. H., Kollonitsch, V., and Kline, C. H., *Ind. Eng. Chem.* **60,** 11 (1968).
13. Masters, C., "Homogeneous Transition-Metal Catalysis," p. 196. Chapman & Hall, London, 1981.
14. Johnson, M. F. L., and LeRoy, V. M., *J. Catal.* **35,** 434 (1974).
15. Webb, A. N., *J. Catal.* **39,** 485 (1975).
16. Hurst, N. W., Gentry, S. J., Jones, A., and McNicol, B. D., *Catal. Rev.* **24,** 233 (1982).
17. Bolivar, C., Charcosset, H., Frety, R., Primet, M., Tournayan, L., Betizeau, C., Leclercq, G., and Maurel, R., *J. Catal.* **39,** 249 (1975).
18. Yao, H. C., and Shelef, M., *J. Catal.* **44,** 392 (1976).
19. McNicol, B. D., *J. Catal.* **46,** 438 (1977).
20. Wagstaff, N., and Prins, R., *J. Catal.* **59,** 434 (1979).
21. Isaacs, B. H., and Petersen, E. E., *J. Catal.* **77,** 43 (1982).
22. Wang, L., and Hall, W. K., *J. Catal.* **82,** 177 (1983).
23. Duchet, J. C., van Oers, E. M., de Beer, V. H. J., and Prins, R., *J. Catal.* **80,** 386 (1983).
24. Thomas, R., van Oers, E. M., de Beer, V. H. J., and Moulijn, J. A., *J. Catal.* **84,** 275 (1983).
25. Klug, H. P., and Alexander, L. E., "X-Ray Diffraction Procedures," p. 491. Wiley, New York, 1954.
26. Arnoldy, P., and Moulijn, J. A., *J. Catal.* **93,** 38 (1985).
27. Krebs, B., Müller, A., and Beyer, H. H., *Inorg. Chem.* **8,** 436 (1969).
28. Beyer, H., Glemser, O., Krebs, B., and Wagner, G., *Z. Anorg. Allg. Chem.* **376,** 87 (1970).
29. Martens, H., and Ziegenbalg, S., *Z. Anorg. Allg. Chem.* **401,** 145 (1973).
30. Baker, R. T. K., Chludzinski, J. J., Jr., Dispenziere, N. C., and Murrell, L. L., "Proceedings, 16th Biennial Conference on Carbon", p. 164. American Carbon Society, California, 1983.
31. Wigmans, T., and Moulijn, J. A., *in* "Proceedings, 7th International Congress on Catalysis, Tokyo, 1980" (T. Seiyama and K. Tanabe, Eds.), p. 501. Elsevier, Amsterdam, 1981.
32. Wigmans, T., Auwerda, K., and Moulijn, J. A., 'Proceedings, 6th London International Carbon and Graphite Conference," p. 172. Society of Chemical Industry, London, 1982.
33. Wigmans, T., van Doorn, J., and Moulijn, J. A., *Surf. Sci.* **135,** 532 (1983).
34. Wimmers, O. J., Arnoldy, P., and Moulijn, J. A., submitted for publication.
35. Arnoldy, P., Bruinsma, O. S. L., and Moulijn, J. A., *J. Mol. Catal.* **30,** 111 (1985).
36. Olsthoorn, A. A., and Boelhouwer, C., *J. Catal.* **44,** 197 (1976).
37. D'Aniello, M. J., *J. Catal.* **69,** 9 (1981).
38. Wang, L., and Hall, W. K., *J. Catal.* **77,** 232 (1982).
39. Evans, M., and Marsh, H., *in* "Characterisation of Porous Solids" (S. J. Gregg, K. S. W. Sing, and H. F. Stoeckli, Eds.), p. 53. Society of Chemical Industry, London, 1979.
40. Shpiro, E. S., Avaev, V. I., Antoshin, G. V., Ryashentseva, M. A., and Minachev, Kh.M., *J. Catal.* **55,** 402 (1978).
41. Johnson, M. F. L., *J. Catal.* **39,** 487 (1975).